4

Mean State and the MJO in a High Resolution Nested Regional Climate Model

Pallav Ray
International Pacific Research Center (IPRC), University of Hawaii
USA

1. Introduction

The Madden-Julian oscillation (MJO, Madden and Julian, 1971, 1972) is a dominant feature of intraseasonal (20-90 day) variability in the tropics. According to the classic view, the MJO begins as a positive convective anomaly in the equatorial western Indian Ocean. It then propagates eastward toward the maritime continent where convection weakens until the MJO reaches the west Pacific where the convection strengthens again. Convective coupling diminishes in the eastern Pacific in the presence of cooler sea surface temperature (SST), but the wind component in the upper troposphere may propagate eastward as free waves at about 12-15 m s^{-1}, much faster than the MJO propagation speed of 5 m s^{-1} (Knutson et al., 1986). Global circumnavigation associated with the MJO can also be noticed in the upper-tropospheric divergent wind (e.g., Krishnamurti et al., 1985; Knutson and Weickman, 1987) and moisture fields (Kikuchi and Takayabu, 2003), but is difficult to detect in parameters closer to the surface.

The MJO has been found to influence a number of features in the tropics including the Indian summer monsoon (e.g., Yasunari, 1979), Australian monsoon (e.g., Hendon and Liebmann, 1990), tropical storms (e.g., Liebmann et al., 1994), and the initiation of El Nino events (e.g., Lau and Chan, 1985). However, the influence of the MJO is not limited to the tropics. The MJO affects the global medium and extended range weather forecasts (e.g., Jones and Schemn, 2000) and modulates the global angular momentum (e.g., Weickmann et al., 1997). This tropics-extratropics interaction produced by the MJO affects the skill of the northern hemisphere weather forecasts (Ferranti et al., 1990). The long periodicity of the MJO convection relates it with the predictability on seasonal time scales. As a result, longer-range forecasts could be improved if the MJO can be predicted.

There have been considerable advancements in understanding the different aspects of the MJO using observation, theory and numerical modeling. However, an accurate MJO simulation using numerical models remains an extremely difficult task due to a number of model deficiencies (Lin et al., 2006; Zhang et al., 2006; Kim et al., 2009). One such deficiency is the model's inability in capturing the correct mean state. The role of the mean state on the MJO was previously explored using GCMs (e.g., Slingo et al., 1996; Inness et al., 2003; Maloney and Hartmann, 2001; Ajayamohan and Goswami, 2007; Maloney, 2009), observations (Zhang and Dong, 2004), and model-observation comparison (Zhang et al., 2006). It is found that the realistic distributions of precipitation, lower-tropospheric zonal

wind and specific humidity, and boundary-layer moisture convergence in models are essential for them to reproduce realistic statistics of the intraseasonal variability. On the other hand, MJO events that are initiated by the extratropical influences may have less dependence on the mean state (e.g., Ray et al., 2011). A review of our present understanding of the MJO can be found in Zhang (2005).

The objective of this chapter is to further explore the role of the mean state on the MJO using a high-resolution nested regional climate model (NRCM). We use the NRCM (http://www.nrcm.ucar.edu), based on the Weather Research and Forecasting Model (WRF). The domain of this NRCM is global (periodic) in the zonal direction and is bounded in the meridional direction. The main advantage of the NRCM compared to a regular regional model is that, without the east-west boundaries, it isolates the external influences arriving solely from the extratropics. The added constraint provided by the lateral boundary conditions is expected to improve the simulated MJO statistics. Also, compared to a GCM, the NRCM has higher resolution and sophisticated physics that may be helpful to better capture the multi-scale organized convection associated with the MJO (Chen et al., 1996; Houze, 2004; Moncrieff, 2010).

The strategy of this study is to integrate the NRCM for several years and evaluate the role of the mean state on the MJO statistics. Our goal is to provide unique perspectives to the MJO dynamics and mean state.

Section 2 describes the configuration of the model, method and data. Section 3 explores the atmospheric mean state and its role on the MJO with an emphasis on the roles played by the mean precipitation and zonal winds at the 850 hPa (U850). Section 4 summarizes the results along with the implications and limitations of this study.

2. Model and data

2.1 Model

We use the NRCM based on the WRF model that was developed at the National Center for Atmospheric Research (NCAR). This is also known as a tropical channel model (TCM), since the model's computational domain is global (periodic) in the zonal direction. Conceptually, the configuration is similar to the TCM developed at the University of Miami based on the fifth-generation Pennsylvania State University-NCAR Mesoscale Model (MM5, Dudhia, 1993; Grell et al., 1995), known as the Tropical MM5 (TMM5, Ray et al., 2009; Ray and Zhang, 2010). The NRCM is atmosphere only and employs Mercator projection centered at the equator with open boundaries in the North-South direction. Global reanalyses data are used to provide the initial and boundary conditions for the model (see section 2.3).

The horizontal resolution of the NRCM is 36 km, and the meridional boundaries are placed at 30°S and 45°N. The model top is at 50 hPa, and 35 vertical levels are used. Output is taken every 3 hours. Based on a series of tests, the suite of parameterizations used for this study are: Kain-Fritsch cumulus parameterization (KF, Kain, 2004), WSM6 cloud microphysics (Hong et al., 2004), CAM 3.0 radiation scheme (Collins et al., 2006), YSU boundary layer scheme (Hong et al., 2006), and Noah land surface model (Chen and Dudhia, 2001). The model was integrated for 5 years from January 1, 1996 to January 1, 2000.

2.2 Method

The NRCM simulation is used to document the mean state and the MJO statistics. The MJO is defined as a planetary scale (zonal wavenumber 1 to 5), eastward propagating, intraseasonal (20-90 day) components in the U850 coupled with precipitation (P). To extract the coupled MJO signal, a singular vector decomposition (SVD) method (Wallace et al., 1992) is applied to U850 and P. This method is similar to EOF analysis, but with one advantage: it considers the wind-precipitation coupling associated with the MJO. The leading modes are selected based on North et al. (1982) rule. Three leading modes are found for both observations and model, and they explain 41% and 31% of the covariance for the observation and the NRCM, respectively. These selected modes represent the intraseasonal coupled components between U850 and P. Time series of U850 and P reconstructed through linear regression of intraseasonal bandpass filtered U850 and P upon their selected leading SVD modes, are considered to represent the MJO. Hereafter, they are referred to as U850* and P*.

2.3 Data

Model validation uses observations and reanalyses data. They include: National Centers for Environmental Prediction-National Center for Atmospheric Research (NCEP-NCAR) Re-analysis (Kalnay et al., 1996) winds and the merged analysis of precipitation (CMAP; Xie and Arkin, 1997).

The initial and boundary conditions of the NRCM are from the NCEP-NCAR reanalysis. The SSTs are from Atmospheric Model Intercomparison Project (AMIP; 1° x 1°, 6-hourly; Taylor et al., 2000). For brevity, both reanalysis and CMAP precipitation will be referred to as "observations".

3. Results

The simulated mean state is described first, followed by the MJO and how it has been affected by the model mean state.

3.1 Mean state

The mean state of the model is compared with the observation with respect to P and U850 (Fig. 1). The main error in the model precipitation is over the equatorial Indian and west Pacific Ocean and over the South Pacific Convergence Zone (SPCZ), where the variance of the MJO related precipitation is maximum (Zhang and Dong, 2005). This is the first indication that the simulated MJO may be affected by the mean state. The model precipitation seems to move further from the equator with much higher values over the southern Indian Ocean and north of maritime continent. Most of this error comes during the northern winter. On the other hand, simulated U850 is somewhat stronger than those of reanalysis over the Indian Ocean and the eastern and central Pacific. The model overestimates winds at 200 hPa in the equatorial Indian and west Pacific Ocean also (not shown). The simulation captures the winds quite well over the west African monsoon region, where the lack of precipitation in the model is obvious. Easterlies at 850 hPa are stronger over the southern Indian Ocean, where there is error in precipitation as well.

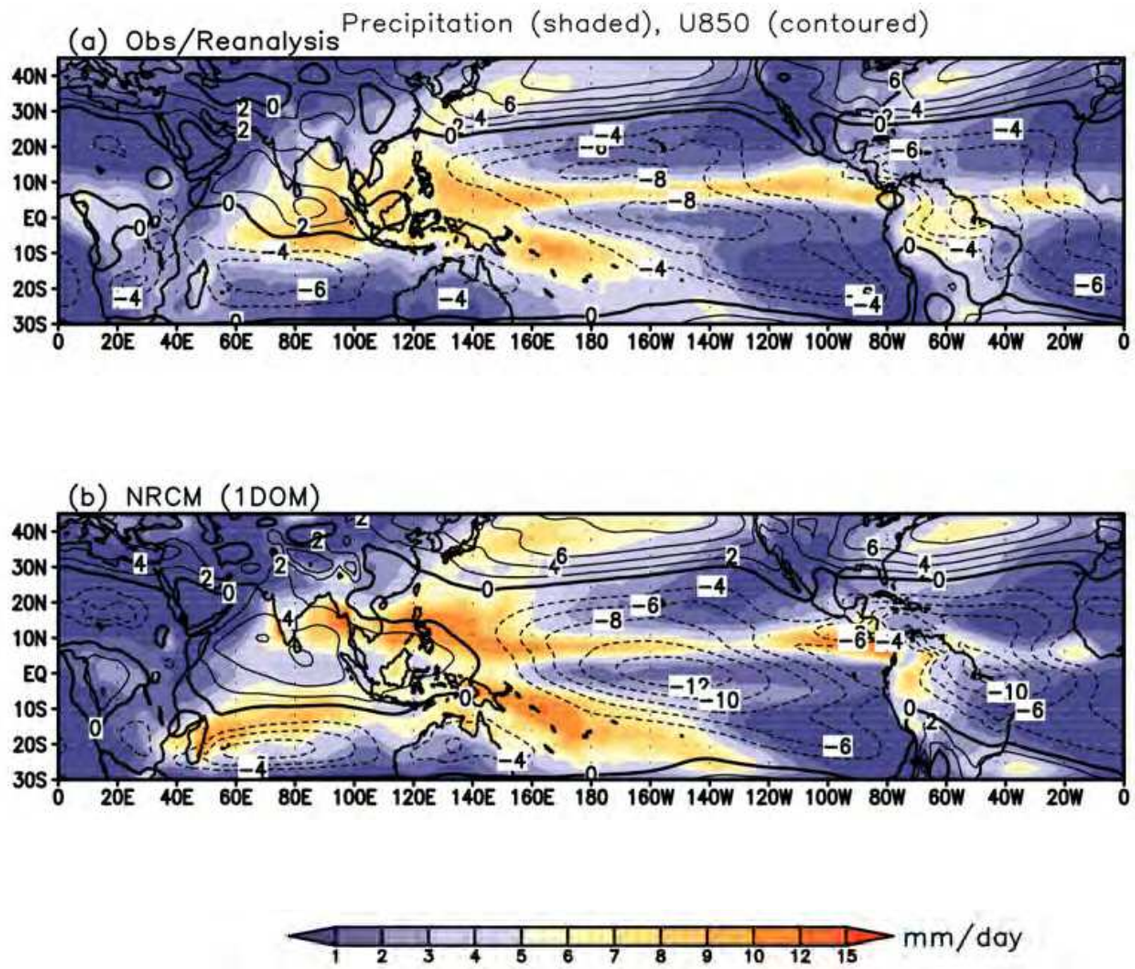

Fig. 1. Annual mean rainfall (shaded, mm/day) and U850 (contoured, m/s) during 1996-2000 from the (a) observation/reanalysis, and (b) NRCM. Zero contours are thickened.

Overall, the precipitation is underestimated over the equatorial (10°S-10°N) Indian Ocean, and is slightly overestimated over the west Pacific (Fig. 2a). However, U850 is overestimated over the Indian Ocean and is slightly underestimated over the west Pacific (Fig. 2b). The results indicate a possible lack of coupling between the winds and precipitation in the model compared to observations.

To further explore the simulated mean state, we show latitudinal distributions of P and U850 in Fig. 3. Precipitation is underestimated close to the equator (10°S-10°N), however, the model overestimates precipitation between 10°-30° latitudes, particularly in the southern hemisphere. The northern ITCZ is shifted towards the higher latitude. As expected, simulated winds are almost same as that of the reanalysis near the boundaries (Fig. 3b). Although there are large differences between the simulated and observed U850 over the equatorial Indian and west Pacific (Fig. 2b), the zonally averaged U850 match well due to the cancellation of errors (Fig. 3b).

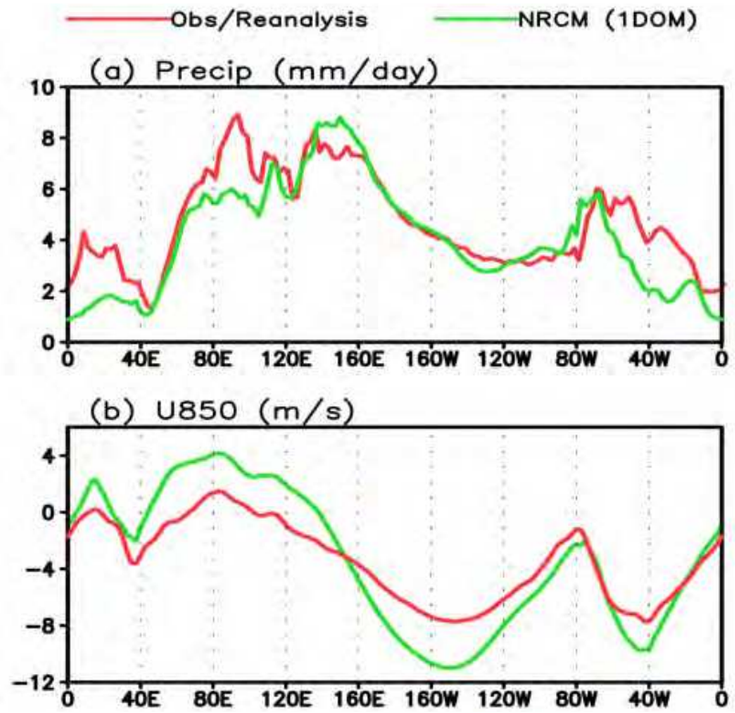

Fig. 2. Longitudinal distribution of (a) Precipitation (mm/day) and (b) U850 (m/s), averaged over 10°S-10°N from the observation/reanalysis (red) and NRCM (green).

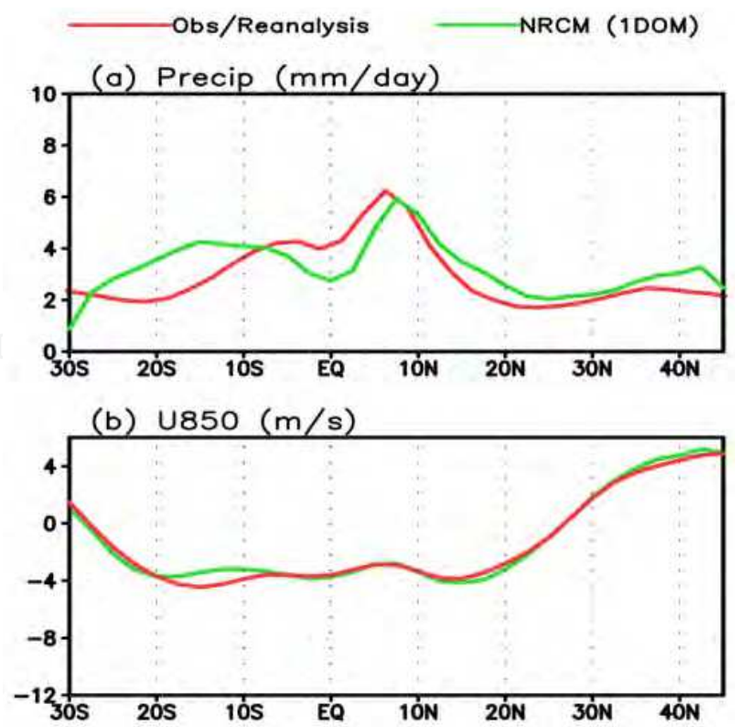

Fig. 3. Latitudinal distribution of (a) Precipitation (mm/day) and (b) U850 (m/s), averaged over 0°-360° from the observation/reanalysis (red) and NRCM (green).

3.2 MJO

A space-time spectrum analysis is performed on the filtered time series of U850 and P to compare the eastward and westward propagating intraseasonal (20-90 day) signal (Fig. 4). A necessary criterion for the MJO is the dominance of the eastward propagating power over its westward propagating counterpart at the intraseasonal and planetary scales. In the observations (Fig. 4, left), the eastward spectral power dominates its westward counterpart at the MJO space and time scales, but not quite so in the simulation (Fig. 4, right), particularly for P (Fig. 4d). The simulated MJO signal in P (Fig. 4d) is much weaker than that in U850 (Fig. 4c) in comparison to the observation. This discrepancy indicates a lack of physical-dynamical coherence in the NRCM simulation. This is consistent with the mean U850 and P in Fig. 1. The results are similar using other variables.

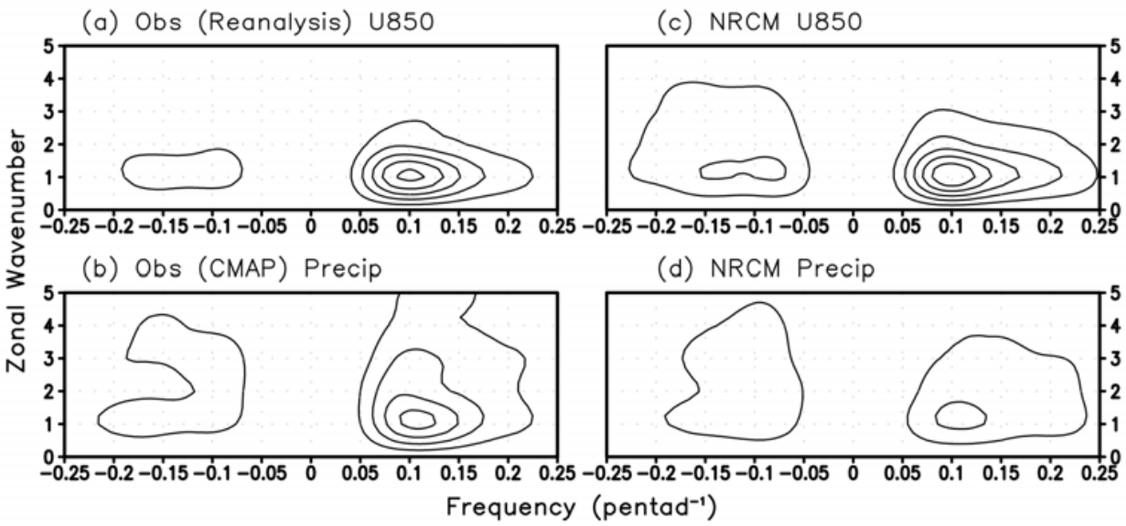

Fig. 4. Time-Space spectra for (a) U850 and (b) precipitation from the observation. The right panels are for the model. Zonal wavenumber 1, and frequency 0.1 (50 days), represent the dominant MJO scales. All are averaged over 10°S-10°N.

To further explore the MJO in the NRCM, the longitudinal variation of the MJO variance of U850 and P are shown in Fig. 5. For U850, over the Indian Ocean, the variance is underestimated, particularly near the equator (5°N-5°S, Fig. 5, right). However, when a larger area is considered (15°S-15°N, Fig. 5, left), the differences between the observation and the model become smaller. Over the west Pacific, however, the model overestimates the MJO variance in U850. For P, the MJO variance is greatly underestimated over the Indian Ocean (Fig. 6), particularly over the western Indian Ocean, where most MJO initiation occurs. This is consistent with the lack of precipitation over the equatorial Indian and west Pacific Ocean as shown in Fig. 1.

It is natural to enquire how the MJO simulation in the NRCM compares with those in GCM simulations. A quick comparison with GCM simulations reveals that the MJO in the NRCM is not better than those in GCMs. This is less than satisfactory considering that the model is forced by time-varying reanalysis boundary conditions. As a result, we further diagnoss the role of the mean state in the simulated MJO statistics.

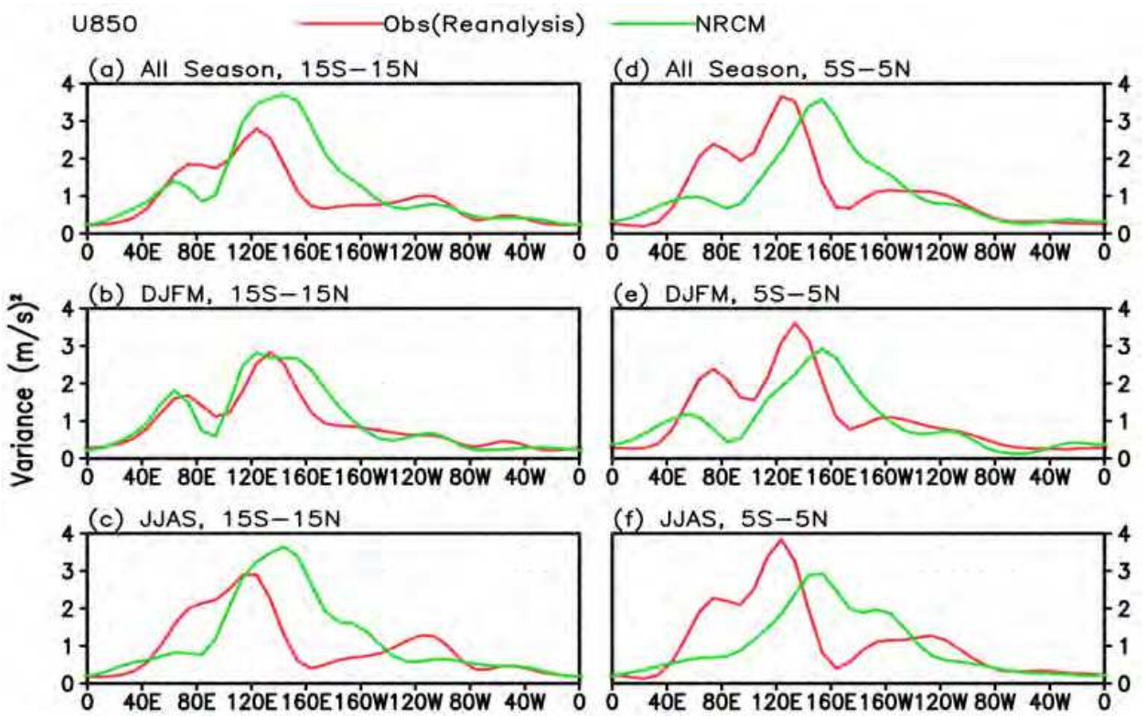

Fig. 5. (left) Variance of U850 averaged over 15°S-15°N during (a) all season, (b) boreal winter (DJFM), and (c) boreal summer (JJAS). Right panels are averaged over 5°S-5°N.

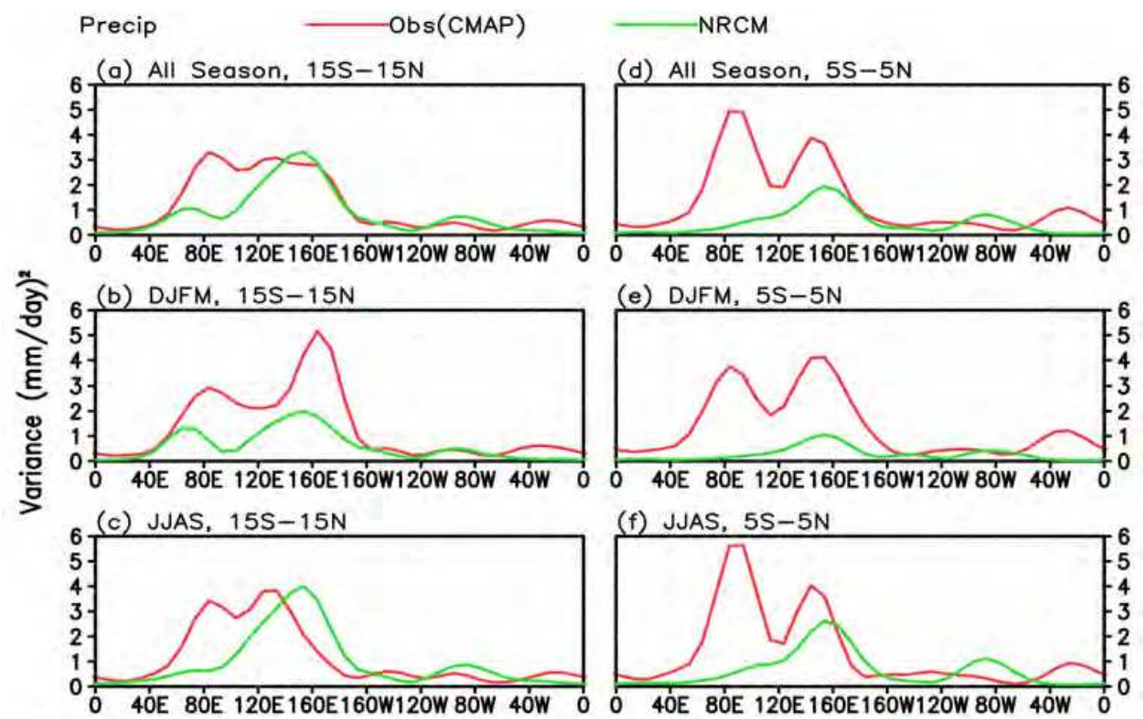

Fig. 6. (left) Variance of P averaged over 15°S-15°N during (a) all season, (b) boreal winter, and (c) boreal summer. Right panels are averaged over 5°S-5°N.

3.3 Role of the mean state on the MJO

Role of the mean state on the simulated MJO is described with respect to U850 and Precipitation. The MJO is represented by the variances of U850* and P*. Figs. 7 and 8 show the role of mean U850 on the U850* variance from the observation and model, respectively. The MJO variance (contoured) and the westerlies (yellow hues) are reasonably collocated in the reanalysis (Fig. 7), but not quite as well in the NRCM (Fig. 8), particularly over the equatorial Indian Ocean. During the boreal winter, simulated westerlies and the MJO variance (Fig. 8a) are stronger and located further from the equator compared to the reanalysis (Fig. 7a). This is the season when the MJO is strongest (Zhang and Dong, 2004). During the boreal summer, the observed variance of the MJO is located north of the equator (Fig. 7b). The simulated variance during the summer in the northern Indian Ocean is greatly reduced in the simulation (Fig. 8b).

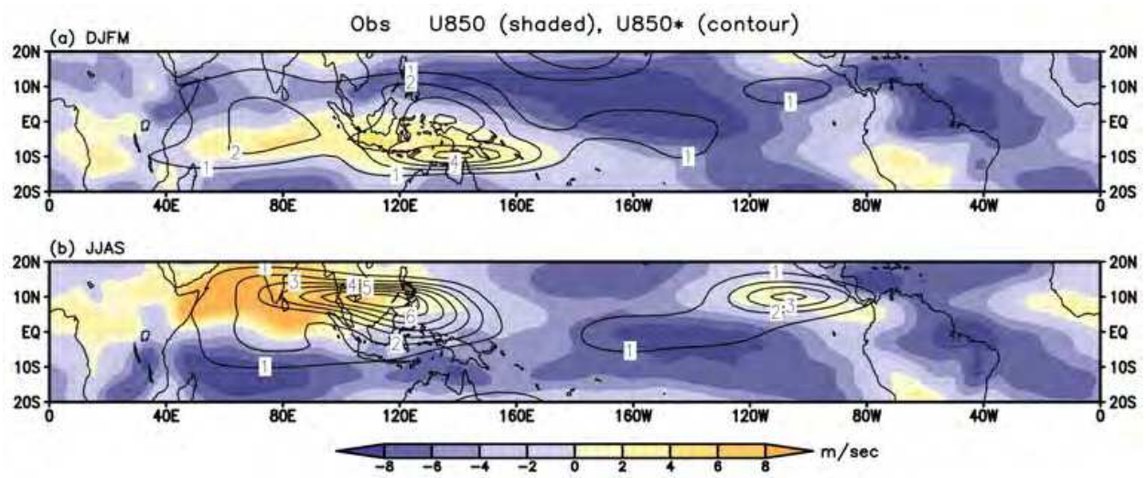

Fig. 7. Mean U850 (m s^{-1}, shaded) and variance of U850* (m^2 s^{-2}, contoured) from the NCEP-NCAR reanalysis during the (a) boreal winter (DJFM), and (b) boreal spring (JJAS). Contour intervals are 1 m^2 s^{-2}.

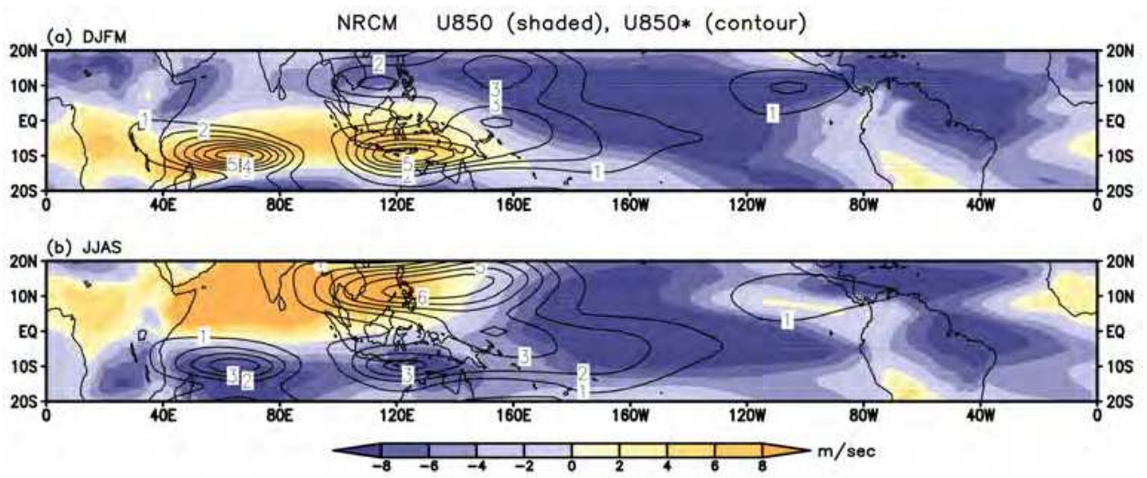

Fig. 8. Same as Fig. 7, but for the model.

Fig. 9 shows the role of the observed mean precipitation on the P* variance. During the boreal winter (Fig. 9a), the P* variance is over the southern hemisphere with three peaks, one over the Indian Ocean, and the other two over the west Pacific. The P* variance is always very well collocated with the stronger mean precipitation. This cannot be said for the NRCM simulation (Fig. 10a), in particular, the P* variance seems to avoid the equator. During the summer, the observed P* variance is in the northern hemisphere (Fig. 9b), however the model produces spurious variance in the SPCZ region and the eastern Pacific. Note that the P* variance is very small over the equatorial Indian Ocean due to the lack of precipitation in that region in the model. This is consistent with the mean annual precipitation (Fig. 1) and the spectrum (Fig. 4) indicating the role of the mean state on the simulated MJO. Next, we describe how the P* variance is affected by the mean distribution of U850.

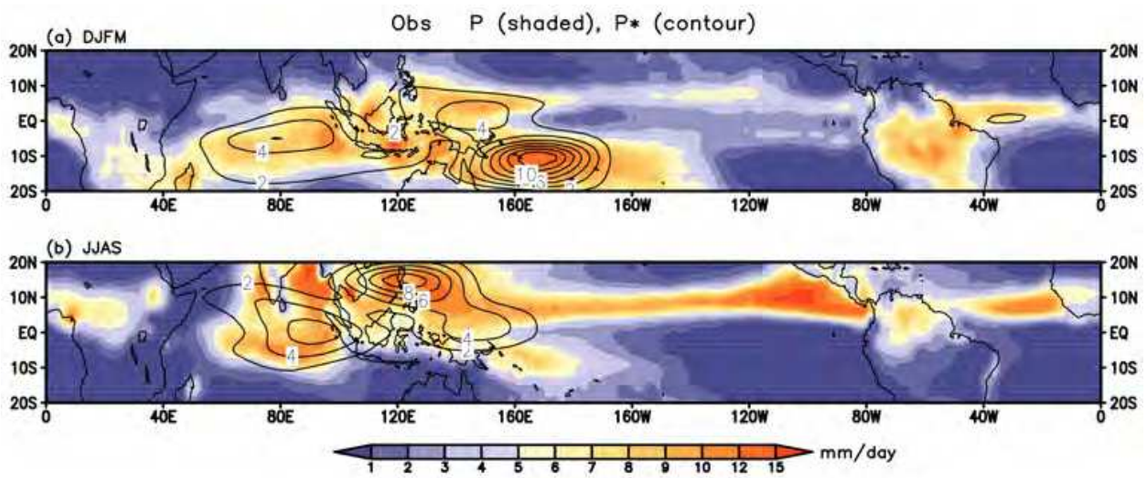

Fig. 9. Mean P (mm day^{-1}, shaded) and variance of P* (mm^2 day^{-2}, contoured) from the observation (CMAP) during the (a) boreal winter (DJFM), and (b) boreal spring (JJAS). Contour intervals are 2 mm^2 day^{-2}.

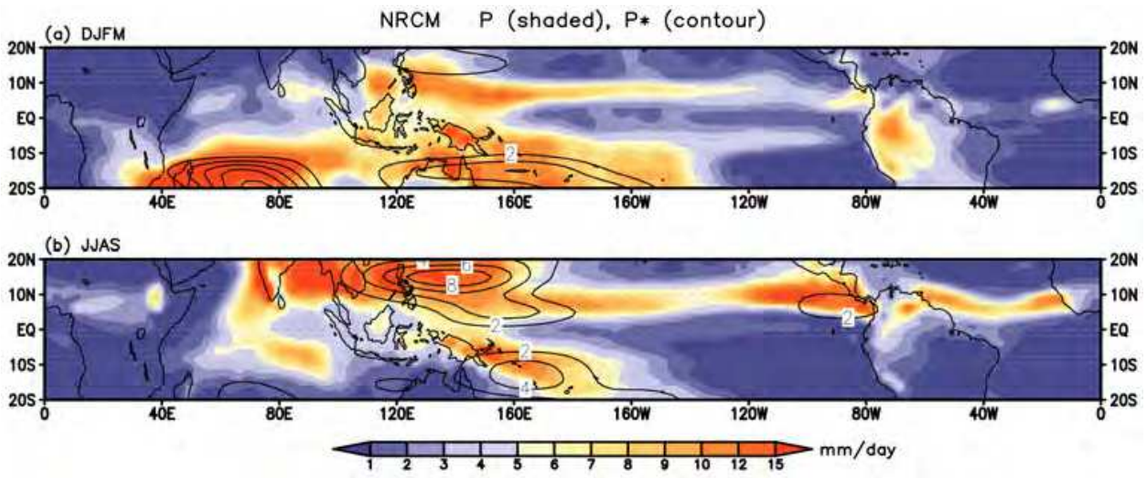

Fig. 10. Same as Fig. 9, but for the model.

Fig. 11 shows the distribution of observed P* variance (contoured) and the mean U850 (shaded). The observed P* maxima always follow the positive U850 or very weak zonal flow in both seasons. Latitudinal migration of mean U850 and P* are more prominent over the west Pacific than over the Indian Ocean. The amplitude of variance is also larger over the west Pacific. The model, however, does not reproduce the observation well (Fig. 12). Variance of P* seems to avoid the westerlies in both seasons. This is one of the most disturbing aspects of the simulated MJO in the NRCM. The larger values of P* variance avoids the equatorial region in the simulation. During the boreal summer, the model reproduces spurious P* variance over the eastern Pacific and in the SPCZ region (Fig. 12b) that is absent in the observation (Fig.11b). It seems that P* variance follows the mean precipitation (Fig. 10), and not the mean westerlies. This indicates a lack of coupling between the convection and circulation in the model.

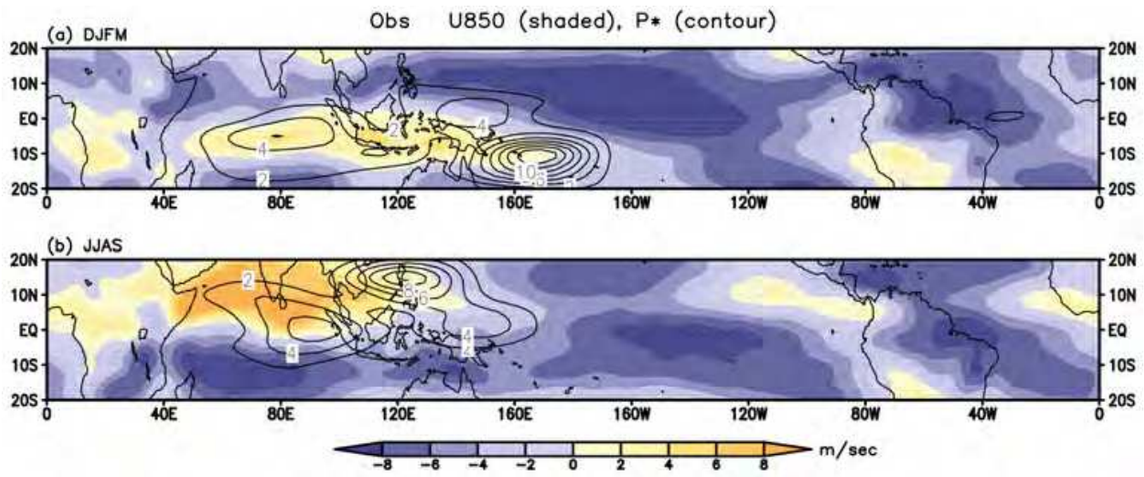

Fig. 11. Mean U850 (m sec^{-1}, shaded) and variance of P* (mm^2 day^{-2}, contoured) from the observation during the (a) boreal winter (DJFM), and (b) boreal spring (JJAS). Contour intervals are 2 mm^2 day^{-2}.

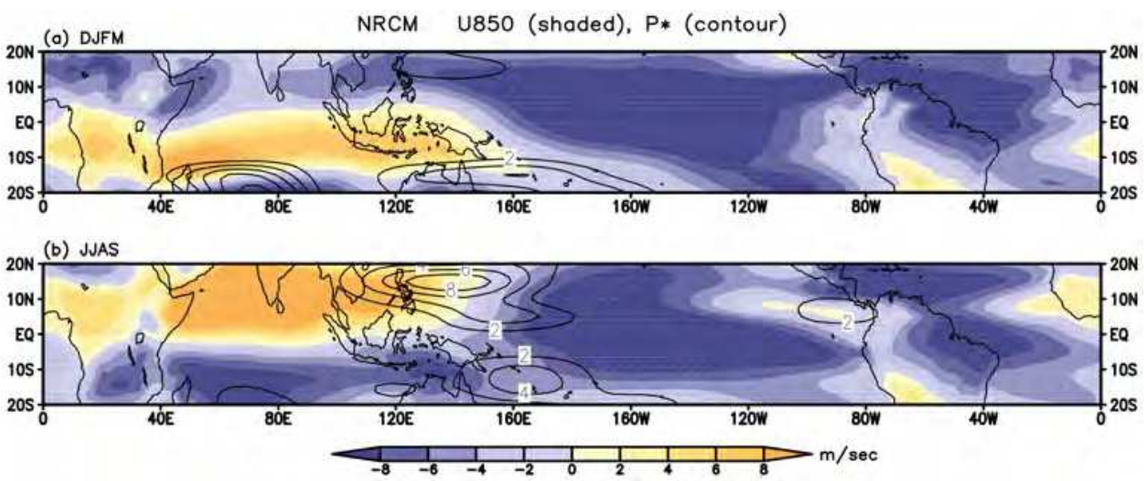

Fig. 12. Same as Fig. 11, but for the model.

4. Conclusion

A nested regional climate model (NRCM) is constructed at the NCAR based on Weather Research and Forecasting (WRF) model. This is also known as a tropical channel model (TCM), and is conceptually similar to the TCM developed at the University of Miami based on MM5. Both TCMs are useful tools to study the MJO dynamics and its initiation.

With the initial and lateral boundary conditions provided by a global reanalysis, the NRCM is integrated for several years. The simulated MJO statistics in the NRCM are not better than those found in the GCMs. This is less than satisfactory considering that the model is forced by time-varying reanalysis boundary conditions. Further diagnoses reveal that the error in the mean state is a reason for the poor MJO statistics in the simulation. For example, the MJO variance and the westerlies in the lower-troposphere are well collocated in the reanalysis, but not quite as well in the NRCM, particularly over the equatorial Indian Ocean where the initiation of the MJO events usually occur. The model also lacks precipitation in the equatorial Indian Ocean. The large error in the precipitation (through modifying the latent heating) must have inhibited any dynamical effects from the lateral boundaries from reaching the interior of the domain. Thus, the lateral boundary conditions couldn't participate effectively in simulating the mean conditions.

However, the multi-year simulation with large error in the mean state was able to capture two individual MJO events that were initiated by the extratropical influences (Ray et al., 2011a). In other words, the negative effect of mean state error can be overcome if there are extra dynamical influences, either from the meridional boundary conditions or initial conditions. Note that, it is not known to what extent the error in the mean state inhibits tropical variability, although it is likely to be model dependent.

The large error in the precipitation over the southern Indian Ocean was thought to be due to the interactions between tropical cyclones and the southern boundaries. To rectify this problem, southern boundaries were further moved to 45°S in another experiment. This simulation also has more vertical levels (55 levels instead of 35) and higher model top at 10 hPa level (instead of 50 hPa). However, this did not improve the result significantly, indicating potential problems with the model physics (Tulich et al., 2011; Murthi et al., 2011). Use of nested domains inside the model also did not improve the mean state (Ray et al., 2011).

In a regular regional model, the domain size is vital for the model mean state through the influence of boundary conditions. For example, a small domain may lead to very little "climate error" because the model is fundamentally controlled by its boundary conditions. On the other hand, the mean state in a global model would be less constrained. The NRCM lies between the regular regional model and the global model. Thus, climate drift in the NRCM simulation would not be noticeable in the smaller regional domains used by Gustafson and Weare (2004a, b) and Monier et al. (2009). How much error in the mean state is sufficient to prevent the initiation of an MJO in the model is not known; arguably, it is event dependent. Thus a systematic study for multiple MJO events including several "primary" (no prior MJO, Matthews, 2008) and "successive" (with prior MJO) events is needed to have a better idea of the effect of mean state on the MJO.

Is the poor skill of the NRCM to simulate MJO due to shortcomings from the cumulus parameterization (Park et al. 1990; Raymond and Torres, 1998; Wang and Schlesinger, 1999;

Maloney and Hartmann, 2001)? Or do we need further increase in the model resolution (Hayashi and Golder, 1986; Gualdi et al., 1997; Grabowski and Moncrieff, 2001; Inness et al., 2001; Liess and Bengtsson, 2004)? The use the Betts-Miller-Janjic (Janjic, 1994) scheme did not improve the MJO simulation. Similarly, higher resolution nested domains inside the NRCM made minor differences. Further works need to be done to investigate the roles of cumulus parameterization and horizontal resolution on the simulated MJO.

The lack of MJO in the NRCM does not necessarily imply a lack of tropical-extratropical interaction. For example, if the observed source of perturbations that eventually initiate an MJO event is located inside the model domain, then the lateral boundary conditions may not be effective beyond the MJO predictability limit. As a result, the locations of the meridional boundaries of the NRCM are crucial for capturing the extratropical influences, if any, on MJO dynamics.

The NRCM is an atmosphere only model forced by the SST without true oceanic feedback. Therefore, it is difficult to rule out the role of coupled air-sea feedbacks in modulating the mean state (Hendon, 2000; Zheng et al. 2004; Vitart et al. 2007; Woolnough et al. 2007). Pegion and Kirtman (2008a, b) found that air-sea coupling was responsible for differences in the simulation of the MJO between the coupled and uncoupled models, specifically in terms of organization and propagation in the western Pacific. The role of intraseasonally varying SST was found to be important to the amplitude and propagation of the oscillation beyond the Maritime continent in their model. After removing the intraseasonally varying component in the SST and lateral boundary conditions in MM5, Gustafson and Weare (2004b) found only minor differences in the MJO simulation compared to the simulation forced with observed SST. Ray et al. (2009) also reported that use of constant SST did not influence the MJO initiation in the Indian Ocean. These results indicate that the MJO amplitude and propagation are influenced by the air-sea interactions whose effect is dominant over the Pacific.

In short, we have shown that the erroneous mean state may be responsible for poor MJO simulation in the model. Our results call for further research attention towards using the untapped potential of high-resolution models in the MJO simulation and forecasting.

5. Acknowledgment

Acknowledgment is made to the NCAR, which is sponsored by the National Science Foundation, for making the NRCM model output available. The NCEP-NCAR reanalysis data were taken from the NOAA/CDC.

6. References

Ajayamohan, R.S. & Goswami, B.N. (2007). Dependence of simulation of boreal summer tropical intraseasonal oscillations on the simulation of seasonal mean. *J. Atmos. Sci*., Vol.64, 460-478

Chen, F. & Dudhia, J. (2001). Coupling an advanced land surface-hydrology model with the Penn State-NCAR MM5 modeling system, Part I: Model implementation and sensitivity. *Mon. Wea. Rev*., Vol.129, pp. 569-585

Chen, S.S.; Houze, R.A. & Mapes, B.E. (1996). Mult-scale variability of deep convection in relation to large-scale circulation in TOGA-COARE. *J. Atmos. Sci*., Vol.53, pp. 1380-1409

Collins, W.D.; Bitz, C.M.; Blackmon, M.L.; Bonan, G.B.; Bretherton, C.S.; Carton, J.A.; Chang, P.; Doney, S.C.; Hack, J.J.; Henderson, T.B.; Kiehl, J.T.; Large, W.G.; McKenna, D.S.; Santer, B.D. & Smith, R.D. (2006). The Community Climate System Model: CCSM3. *J. Clim*., Vol.19, pp. 2122-2143

Done, J.M.; Holland, G.J. & Webster, P.J. (2011). The role of wave energy accumulation in tropical cyclogenesis over the tropical north Atlantic. *Clim. Dyn*., Vol.36, pp. 753-767, doi 10.1007/s00382-010-0880-5

Dudhia, J. (1993). A nonhydrostatic version of the Penn State-NCAR Mesoscale Model: Validation tests and simulation of an Atlantic cyclone and cold front. *Mon. Wea. Rev*., Vol.121, pp. 1493-1513

Ferranti, L.; Palmer, T.N.; Molteni, F. & Klinker, K. (1990). Tropical-extratropical interaction associated with the 30-60 day oscillation and its impact on medium and extended range prediction. *J. Atmos. Sci*., Vol.47, pp. 2177-2199

Grell, G.A.; Dudhia, J. & Stauffer, D.R. (1995). A description of the fifth-generation Penn-State/NCAR Mesoscale Model (MM5). *NCAR/TN-398*.

Grabowski, W.W. & Moncrieff, M.W. (2001). Large-scale organization of tropical convection in two-dimensional explicit numerical simulations. *Quart. J. Roy. Meteor. Soc*., Vol.127, pp. 445-468

Gualdi, S. ; Navarra, A. & Von Starch, H. (1997). Tropical intraseasonal oscillation appearing in operational analyses and in a family of general circulation models. *J. Atmos. Sci*., Vol.54, pp. 1185-1202

Gustafson, W.I. & Weare, B.C. (2004a). MM5 modeling of the Madden-Julian oscillation in the Indian and west Pacific Oceans: Model description and control run results. *J. Clim*., Vol.17, pp. 1320-1337

Gustafson, W.I. & Weare, B.C. (2004b). MM5 modeling of the Madden-Julian oscillation in the Indian and west Pacific Oceans: Implications of 30-70 day boundary effects on MJO development. *J. Clim*., Vol.17, pp. 338-1351

Hayashi, Y. & Golder, D.G. (1986). Tropical intraseasonal oscillation appearing in the GFDL general circulation model and FGGE data. Part I : Phase propagation. *J. Atmos. Sci*., Vol.43, pp. 3058-3067

Hendon, H.H. & Liebmann, B. (1990). The intraseasonal (30-50 day) oscillation of the Australian summer monsoon. *J.* Atmos. *Sci*., Vol.47, pp. 2909-2923

Hendon, H.H. (2000). Impact of air-sea coupling on the Madden-Julian Oscillation in a general circulation model. *J. Atmos. Sci*., Vol.57, pp. 3939-3952

Hong, S.-Y.; Dudhia, J. & Chen, S.-H. (2004). A revised approach to ice microphysical processes for the bulk parameterization of clouds and precipitation. *Mon. Wea. Rev*., Vol.132, pp. 103-120

Hong, S.-Y.; Noh, Y. & Dudhia, J. (2006). A new diffusion package with an explicit treatment of entrainment processes. *Mon. Wea. Rev*., Vol.134, pp. 2318-2341

Houze, R.A. (2004). Mesoscale convective systems. *Rev. Geophys*., Vol.42, RG4003, doi:10.1029/2004RG000150

Inness, P.M.; Slingo, J.M.; Woolnough, S.J.; Neale R.B. & Pope, V.D. (2001). Organization of tropical convection in a GCM with varying vertical resolution: Implications for the simulation of the Madden-Julian oscillation. *Clim. Dyn*., Vol.17, pp. 777-793

Inness, P.M.; Slingo, J.M.; Guilyardi, E. & Cole, J. (2003). Simulation of the Madden-Julian oscillation in a coupled general circulation model. Part II: The role of the basic state. *J. Clim*., Vol.16, 365-382

Janjic, Z.I. (1994). The step-mountain coordinate model: Further development of the convection, viscous sublayer, and turbulence closure schèmes. *Mon. Wea. Rev*., Vol.122, pp. 927-945

Jones, C., & Schemn, J.-K.E. (2000). The influence of intraseasonal variations on medium-range weather forecasts over South America. *Mon. Wea. Rev*., Vol.128, pp. 486-494

Kain, J.S. (2004). The Kain-Fritsch convective parameterization: An update. *J. Appl. Meteorol*., Vol.43, pp. 170-181

Kalnay, E. & Coauthors (1996). The NCEP-NCAR 40-year reanalysis project. *Bull. Amer. Meteor. Soc*., Vol.77, pp. 437-471

Kikuchi K. & Takayabu, Y.N. (2003). Equatorial circumnavigation of moisture signal associated with the Madden-Julian Oscillation (MJO) during boreal winter. *J. Met. Soc. Jpn*., Vol.81, No.4, pp. 851-869

Kim, D. & Coauthors (2009). Application of MJO simulation diagnostics to climate models. *J. Clim*., Vol.22, pp. 6413-6436

Knutson, R.R.; Weickmann, K.M. & Kutzbach, J.E. (1986). Global-scale intraseasonal oscillations of outgoing longwave radiation and 250 mb zonal wind during northern hemisphere summer, *Mon. Wea. Rev*., Vol.114, pp. 605-623

Knutson, R.R. & Weickmann, K.M. (1987). 30-60 day atmospheric oscillations: Composite life-cycles of convection and circulation anomalies. *Mon. Wea. Rev*., Vol.115, pp. 1407-1436

Krishnamurti, T.N.; Jayakumar, P.K.; Sheng, J.; Surgi, N. & Kumar, A. (1985). Divergent circulations on the 30 to 50 day time scale, *J. Atmos. Sci*., Vol.42, pp. 364-375

Lau, K.–M. & Chan, P.H. (1985). Aspects of the 40-50 day oscillation during the northern winter as inferred from outgoing longwave radiation, *Mon. Wea. Rev*., Vol.113, pp. 1889-1909

Liebmann, B.; Hendon, H.H. & Glick, J.D. (1994). The relationship between tropical cyclones of the western Pacific and Indian Oceans and the Madden-Julian Oscillation, *J. Meteor. Soc. Jpn*., Vol.72, pp. 401-411

Liess, S. & Bengtsson, L. (2004). The intraseasonal oscillation in ECHAM4 part II: Sensitivity studies. *Clim. Dyn*., Vol.22, pp. 671-688, doi :10.1007/s00382-004-0407-z

Lin, J.-L., & Coauthors (2006). Tropical intraseasonal variability in 14 IPCC AR4 climate models. Part I: Convective signals. *J. Clim*., Vol.19, pp. 2665-2690

Madden, R.A. & Julian, P.R. (1971). Detection of a 40-50 day oscillation in the zonal wind in the tropical Pacific. *J. Atmos. Sci*., Vol.28, pp. 702-708

Madden, R.A. & Julian, P.R. (1972). Description of global-scale circulation cells in the tropics with a 40-50 day period. *J. Atmos. Sci*., Vol.29, pp. 1109-1123

Maloney, E.D. (2009). The moist static energy budget of a composite tropical intraseasonal oscillation in a climate model. *J. Clim*., Vol.22, pp. 711-729

Maloney, E.D. & Hartman, D.L. (2001). The sensitivity of intraseasonal variability in the NCAR CCM3 to changes in convective parameterization. *J. Clim*., Vol.14, pp. 2015-2034

Matthews, A.J. (2008). Primary and successive events in the Madden-Julian oscillation. *Quart. J. Roy. Meteor. Soc*., Vol.134, pp. 439-453

Moncrieff, M.W. (2010). The multi-scale organization of moist convection and the interaction of weather and climate, In D.-Z. Sun and F. Bryan (Eds.), Climate Dynamics: Why Does Climate Vary? *Geophysical monograph series*, Vol.189, American Geophysical Union, Washington DC, 3-26, doi:10.1029/2008GM000838

Monier, E.; Weare, B.C. & Gustafson, W.I. (2009). The Madden-Julian oscillation wind-convection coupling and the role of moisture processes in the MM5 model. *Clim. Dyn*., doi:10.1007/s00382-009-0626-4

Murthi, A.; Bowmann, K.P. & Leung, L.R. (2011). Simulations of precipitation using NRCM and comparisons with satellite observations and CAM: annual cycle. *Clim. Dyn*. (in press)

North, G.R.; Bell, T.L.; Cahalan, R.F. & Moeng, F.J. (1982). Sampling errors in the estimation of empirical orthogonal functions. *Mon. Wea. Rev*., Vol.110, pp. 699-710

Park, C.-K.; Strauss, D.M. & Lau, K.-M. (1990). An evaluation of the structure of tropical intraseasonal oscillations in three general circulation models. *J. Meteorol. Soc. Jpn*., Vol.68, pp. 403-417

Pegion, K. & Kirtman, B.P. (2008a). The impact of air-sea interactions on the simulation of tropical intraseasonal variability. *J. Clim*., Vol.21, pp. 6616-6635

Pegion, K. & Kirtman, B.P. (2008b). The impact of air-sea interactions on the predictability of tropical intraseasonal variability. *J. Clim*., Vol.21, pp. 5870-5886

Ray, P.; Zhang, C.; Dudhia, J. & Chen S.S. (2009). A numerical case study on the initiation of the Madden-Julian oscillation. *J. Atmos. Sci*., Vol.66, pp. 310-331

Ray, P. & Zhang, C. (2010). A case study of the mechanics of extratropical influence on the initiation of the Madden-Julian oscillation. *J. Atmos. Sci*., Vol.67, pp. 515-528

Ray, P.; Zhang, C.; Moncrieff, M.W.; Dudhia, J., Caron, J., Leung, R. & Bruyere, C. (2011). Role of the atmospheric mean state on the initiation of the Madden-Julian oscillation in a tropical channel model. *Clim. Dyn*., Vol.36, pp. 161-184, doi 10.1007/s00382-010-0859-2

Ray, P., Zhang, C. ; Dudhia, J. ; Li, T. & Moncrieff, M.W. (2012) Tropical channel model, InTech publication, *Climate Models*, ISBN 979-953-307-338-4

Raymond, D.J. & Torres, D.J. (1998). Fundamental moist modes of the equatorial troposphere. *J. Atmos. Sci*., Vol.55, pp. 1771-1790

Slingo, J.M. & Coauthors (1996). Intraseasonal oscillations in 15 atmospheric général circulation models: Results from an AMIP diagnostic subproject. *Clim. Dyn*., Vol.12, pp. 325-357

Taylor, K.E.; Williamson, D. & Zwiers, F. (2000). The sea surface temperature and sea-ice concentration boundary conditions for AMIP II simulations. PCMDI Report No. 60 and UCRL-MI-125597, 25 pp

Tulich, S.N.; Kiladis, G.N. & Suzuki-Parker, A. (2011). Convectively coupled Kelvin and easterly waves in a regional climate simulation of the tropics. *Clim. Dyn*., Vol.36, pp. 185-203, doi 10.1007/s00382-009-0697-2

Vitart, F.; Woolnough, S.J.; Balmaseda, M.A. & Tompkins, A.M. (2007). Monthly forecast of the Madden-Julian oscillation using a coupled GCM. *Mon. Wea. Rev*. Vol.135, pp. 2700-2715

Wallace, J.M. ; Smith, C. & Bretherton, C.S. (1992). Singular value decomposition of wintertime sea surface température and 500-mb height anomalies. *J. Clim*., Vol.5, pp. 561-576

Wang, W.Q. & Schlesinger, M.E. (1999). The dependence on convective parameterization of the tropical intraseasonal oscillation simulated by the Uiuc 11-layer atmospheric GCM. *J. Clim*., Vol.12, pp. 1423-1457

Weickmann, K.; Kiladis G.N., & Sardeshmukh, P. (1997). The dynamics of intraseasonal atmospheric angular momentum oscillations. *J. Atmos. Sci*., Vol.54, 1445-1461

Woolnough, S.J.; Vitart, F. & Balmaseda, M. (2007). The role of the ocean in the Madden-Julian oscillation: sensitivity of an MJO forecast to ocean coupling. *Quart. J. Royal. Meteor. Soc*., Vol.133, pp. 117-128

Xie, P. & Arkin, P.A. (1997). Global precipitation: A 17-year monthly analysis based on gauge observations, satellite estimates, and numerical model outputs. *Bull. Amer. Meteor. Soc*., Vol.78, pp. 2539-2558

Yasunari, T., (1979). Cloudiness fluctuations associated with the Northern Hemisphere summer monsoon, *J. Meteor. Soc. Jpn*., 57, 227-242

Zhang, C. & Dong, M. (2004). Seasonality of the Madden-Julian oscillation. J. *Clim*., Vol.17, pp. 3169-3180

Zhang, C. (2005). Madden-Julian oscillation. *Rev. Geophys*., Vol.43, RG2003, doi:10.1029/2004RG000158.

Zhang, C.; Dong, M.; Gualdi, S.; Hendon, H.H.; Maloney, E.D.; Marshall, A.; Sperber, K.R. & Wang, W. (2006). Simulations of the Madden-Julian oscillation by four pairs of coupled and uncoupled global models. *Clim. Dyn*., DOI: 10.1007/s00382-006-0148-2

Zheng, Y.; Waliser, D.E.; Stern, W.F. & Jones, C. (2004). The role of coupled sea surface temperatures in the simulation of the tropical intraseasonal oscillation. *J. Clim*, Vol.17, pp. 4109-4134

Atmospheric Model Applications

Edited by Dr. Ismail Yucel

ISBN 978-953-51-0488-9
Hard cover, 296 pages
Publisher InTech
Published online 04, April, 2012
Published in print edition April, 2012

This book covers comprehensive text and reference work on atmospheric models for methods of numerical modeling and important related areas of data assimilation and predictability. It incorporates various aspects of environmental computer modeling including an historical overview of the subject, approximations to land surface and atmospheric physics and dynamics, radiative transfer and applications in satellite remote sensing, and data assimilation. With individual chapters authored by eminent professionals in their respective topics, Advanced Topics in application of atmospheric models try to provide in-depth guidance on some of the key applied in atmospheric models for scientists and modelers.

InTech Europe
University Campus STeP Ri
Slavka Krautzeka 83/A
51000 Rijeka, Croatia
Phone: +385 (51) 770 447
Fax: +385 (51) 686 166
www.intechopen.com

InTech China
Unit 405, Office Block, Hotel Equatorial Shanghai
No.65, Yan An Road (West), Shanghai, 200040, China
中国上海市延安西路65号上海国际贵都大饭店办公楼405单元
Phone: +86-21-62489820
Fax: +86-21-62489821

IntechOpen